GEORGIA INSTITUTE OF TECHNOLOGY
Engineering Experiment Station

PROJECT INITIATION

Date: Feb. 24, 1969

Project Title: Particle Dynamics in Inertial Fields

Project No.: B-357

Project Director: J. H. Burson

Sponsor: Public Health Service

Effective . . . January 1, 1969 . . . . . Estimated to run until: Dec. 31, 1969 . . . . . .

Type Agreement: . . Grant UI-00414-07 . . . . . Amount: $ 37,954* . . . . . .

Reports: Final Report - Ten (10) copies to Sponsor within six (6) months (6-30-70) after completion

Contact Person: Dr. John E. Lynn, Grants Program Officer
Occupational Safety and Health
Environmental Control Administration
222 East Central Parkway
Cincinnati, Ohio 45202

*Cost-sharing requirements: $1,990.00; Companion Account E-100-405. Total Project Funds $39,944 includes $144 for 06 expenses to be transferred to 07.

Assigned to . . CSMD . . . . . Division

COPIES TO:

- ☐ Project Director
- ☐ Director
- ☐ Associate Director
- ☐ Assistant Director(s)
- ☐ Division Chiefs
- ☐ Branch Head
- ☐ General Office Services
- ☐ Engineering Design Services
- ☐ Photographic Laboratory
- ☐ Research Security Officer
- ☐ Accounting
- ☐ Purchasing
- ☐ Report Section
- ☑ Library
- ☐ Rich Electronic Computer Center
- ☐ _____

GEORGIA INSTITUTE OF TECHNOLOGY
Engineering Experiment Station

PROJECT TERMINATION

Date 5/14/71

PROJECT TITLE: Particle Dynamics in Inertial Fields

PROJECT NO: B-357

PROJECT DIRECTOR: J. H. Burson

SPONSOR: Public Health Service

TERMINATION EFFECTIVE: 9/30/70

CHARGES SHOULD CLEAR ACCOUNTING BY: All charges have cleared.

Obligations Remaining:

Final Report - due 4/30/71.

Chemical Sciences & Materials Division

COPIES TO:

Project Director
Director
Associate Director
Assistant Directors
Division Chief
Branch Head
Accounting
Engineering Design Services
General Office Services
Photographic Laboratory
Purchasing
Report Section
Library ✓
Security
Rich Electronic Computer Center

Form EES 402 (R10-62)

B-357

FINAL REPORT

PROJECT B-357

PARTICLE DYNAMICS IN INERTIAL FIELDS

BY JOHN H. BURSON, III

Grant 8 R01 EC 00210-07

1 January 1967 to 30 September 1970

Prepared for
Department of Health, Education, and Welfare
Public Health Service
Health Services and Mental Health Administration
National Institute for Occupational Safety and Health
Fifth and Walnut Streets
Cincinnati, Ohio 45202

1973

Engineering Experiment Station
GEORGIA INSTITUTE OF TECHNOLOGY
Atlanta, Georgia

GEORGIA INSTITUTE OF TECHNOLOGY
ENGINEERING EXPERIMENT STATION
Atlanta, Georgia 30332

FINAL REPORT

PROJECT B-357

PARTICLE DYNAMICS IN INERTIAL FIELDS

By

JOHN H. BURSON, III

GRANT 8 R01 EC 00210-07

1 JANUARY 1967 to 30 SEPTEMBER 1970

Prepared for

DEPARTMENT OF HEALTH, EDUCATION, AND WELFARE
PUBLIC HEALTH SERVICE
HEALTH SERVICES AND MENTAL HEALTH ADMINISTRATION
NATIONAL INSTITUTE FOR OCCUPATIONAL SAFETY AND HEALTH
FIFTH AND WALNUT STREETS
CINCINNATI, OHIO 45202

I. Introduction

This report summarizes work performed during the latter phases of this grant. Earlier works were reported in a previous comprehensive report and in a series of reports and publications listed in Appendix A.

The major effort during the latter stages of this grant was directed to the development and complete theoretical and experimental characterization of a centrifugal particle classifier that would be effective well into the sub-micron size range. From a practical standpoint, particulates in this size range are very important physiologically. Such a device that would simultaneously collect and classify according to aerodynamic diameters is believed to represent an important advance in particulate technology.

A preliminary study regarding the ballistic trajectories of fine particles and subsequent use of this principle in development of a particle size classifier was also initiated during the last year of this grant. The results of this study were not completed before termination of the grant. Initial results appeared promising, and it is hoped that this novel idea can be further explored in the future.

The investigation of particle size classification based on the difference of deposition angle on the rotor wall of a gas centrifuge under forced vortex conditions at atmospheric pressure has been reported in an earlier report of this grant; however, no studies at reduced pressures have been reported.

With the method of this study, a centrifuge produces centrifugal force fields approximating those of a forced vortex in the classification chamber.

The particles travel from near the center of rotation to the rotor wall. In the classification chamber, the particle motion is delayed by Coriolis' force acting opposite to the direction of rotation, causing a gradation of particle size on the rotor wall. At reduced pressure, the mean free path of the gas molecules is of the same order of magnitude as, or greater than, the particle size. In such a case, the effect of the slip factor in the 'Cunningham correction' is large, and the fine particles in the subsieve and submicron ranges can be classified with good resolution.

A comparison of experimental results with calculated results is presented for experiments at various pressures and using glass beads, zinc powder, plastic powders, and tungsten powder.

Also, studies have been made which indicate excellent particle classification, even at large aerosol flow rates where the theoretical requirements for forced vortex conditions are not precisely met.

II. Experimental Apparatus and Procedure

A schematic sketch of the centrifuge and associated equipment used to investigate particle size classification is shown in Fig. 1. As the centrifuge has a liquid seal on the shaft to make it air-tight, it can be used at reduced pressures.

As shown in Fig. 2, the rotor is made of high-strength aluminum and the classification chamber is 21.4 cm inside diameter and 1.3 cm deep. Two webs are installed in the rotor to ensure forced vortex conditions. The particle inlets to the classification chamber are mounted on the rotor, and rotate at the same angular velocity.

The powder is charged in an acrylic resin tube fitted with a screen

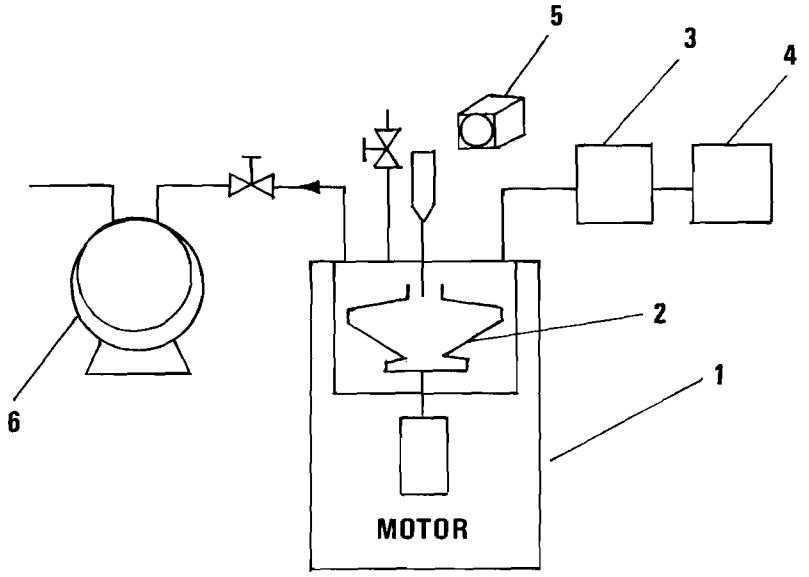

1. CENTRIFUGE
2. ROTOR
3. VACUUM GAUGE
4. RECORDER FOR VACUUM
5. STROBOSCOPE
6. VACUUM PUMP

Figure 1. Scheme of the Experimental Apparatus.

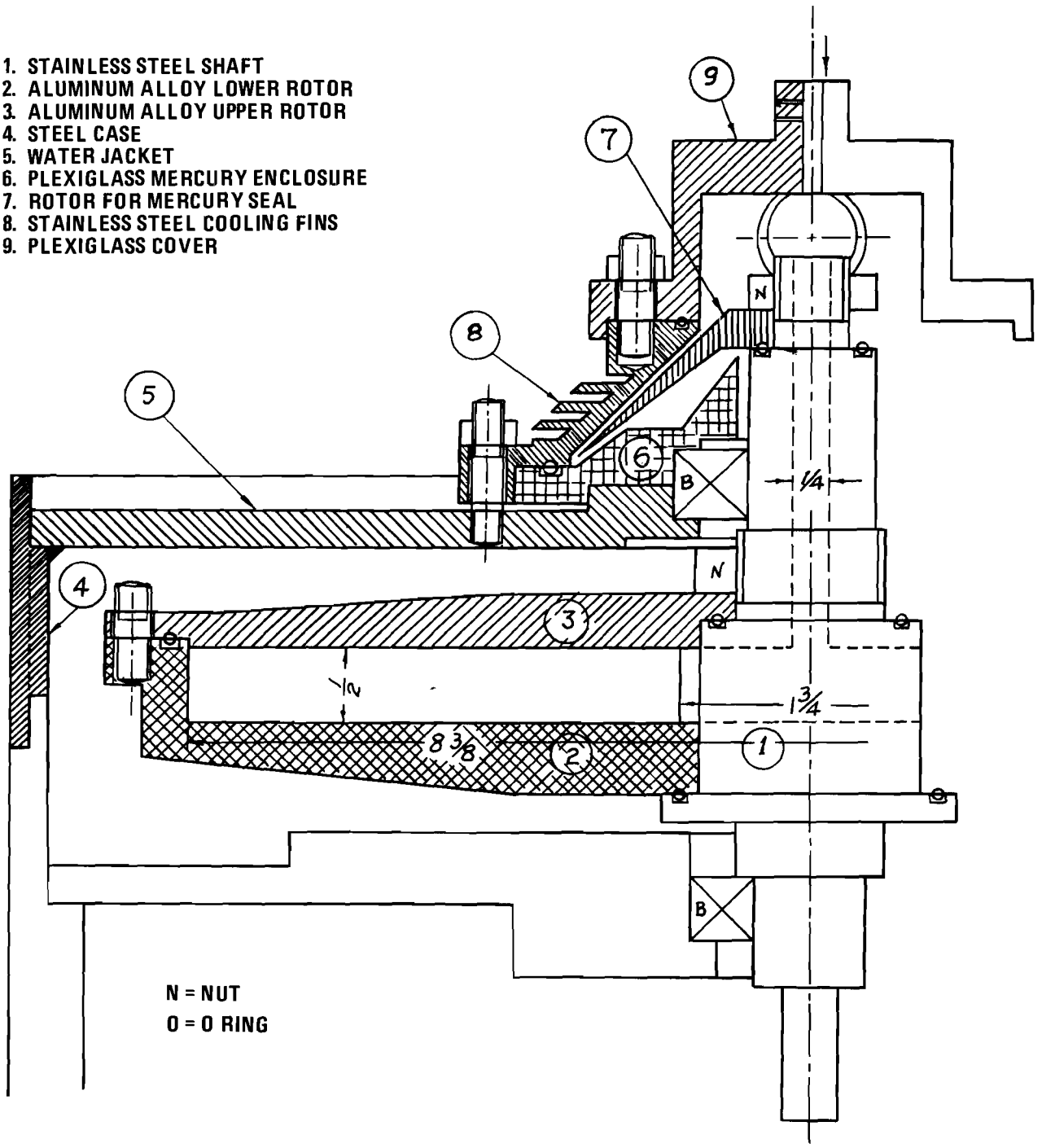

Figure 2. Centrifugal Classifier Capable of Operation at Reduced Pressure.

of 325# or 1000# mesh on the bottom for dispersion. As shown in Fig. 3, this tube is placed inside a glass tube with a rubber seal to make it air tight.

After the centrifuge attains the specified pressure and speed of rotation, a 60Hz vibration is applied to the feeding device to make the particles disperse, pass through the capillary and enter the classification chamber. Hence at the particle inlets, the particles attain essentially the same angular velocity as the rotor.

In the classification chamber, the particles move from near the center (r_o = 1.90) to the rotor wall (r = 8.9). During their trajectories, the particles are classified and deposit on the rotor wall in accordance with the particle size. The motion of the particles relative to the rotor is opposite to the rotation of rotor. The deposition angle, which is the difference between the angular displacement of the rotor and the particle on the rotor wall, that is $(\phi - \theta)\big|_{r=8.9}$, increases with increasing particle size.

Transparent, double-sided adhesive tapes were mounted on 12 mm transparent plastic strips and placed on the rotor wall. In the case of submicron particles, grids for the electron microscope were mounted on these strips.

After centrifuging, the particle sizes and their respective angular locations were determined using an optical or electron microscope.

Glass beads (ρ_p = 2.5g/cm^3), zinc powder (ρ_p = 7.0g/cm^3), plastic beads (ρ_p = 1.0g/cm^3) and tungsten powder (ρ_p = 19.2g/cm^3) were used as the test materials. Hollow particles in the glass beads were removed by flotation with a mixture of acetone and 1,1,2,2-tetrabromoethane.

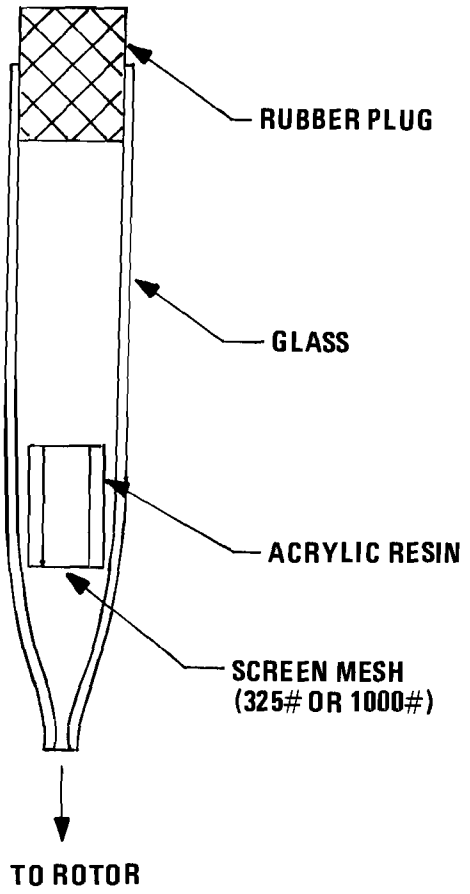

Figure 3. Feeding Device for Powder.

III. Theoretical Considerations

Particle motion in centrifugal fields is always changing with respect to both velocity and direction, that is, the motion is non-uniform and curvilinear. The equations of motion for a spherical particle in polar coordinates are given by the following expression:

$$\frac{\pi}{6} D_p^3 (\rho_p + \tfrac{1}{2}\rho_g)\frac{d^2r}{dt^2} + \frac{C_D}{C_c} \frac{\pi}{8} D_p^2 \rho_g v \frac{dr}{dt} - \frac{\pi}{6} D_p^3(\rho_p + \tfrac{1}{2}\rho_g) r\left(\frac{d\theta}{dt}\right)^2$$

$$+ \frac{\pi}{4} D_p^3 \rho_g r\left(\frac{d\phi}{dt}\right)^2 + \frac{3}{2}\sqrt{\pi\mu\rho_g}\ D_p^2 \int_o^t \left\{\frac{d^2r}{dx^2} - r\left(\frac{d\theta}{dx}\right)^2 + r\left(\frac{d\phi}{dx}\right)^2\right\} \frac{dx}{\sqrt{t-x}} = 0 \qquad (1)$$

$$\frac{\pi}{6} D_p^3(\rho_p + \tfrac{1}{2}\rho_g) r\frac{d^2\theta}{dt^2} + \frac{C_D}{C_c} \frac{\pi}{8} D_p^2 \rho_g v\, r\left(\frac{d\theta}{dt} - \frac{d\phi}{dt}\right) + \frac{\pi}{3} D_p^3(\rho_p + \tfrac{1}{2}\rho_g) \frac{dr}{dt}\frac{d\theta}{dt}$$

$$+ \frac{3}{2}\sqrt{\pi\mu\rho_g}\ D_p^2 \int_o^t \left(r\frac{d^2\theta}{dx^2} + 2\frac{dr}{dx}\frac{d\theta}{dx}\right) \frac{dx}{\sqrt{t-x}} = 0 \qquad (2)$$

in which

$$v = \sqrt{\left(\frac{dr}{dt}\right)^2 + r^2 \left(\frac{d\phi}{dt} - \frac{d\theta}{dt}\right)^2} \qquad (3)$$

$$C_D = \frac{24}{Re}\left(1 + 0.15\ Re^{0.687}\right) \qquad (4)$$

$$Re = \frac{D_p v \rho_g}{\mu} \qquad (5)$$

$$C_c = 1 + \left\{2.46 + 0.82 \exp\left(-\frac{0.44\ D_p}{\lambda_m}\right)\right\} \frac{\lambda_m}{D_p} \qquad (6)$$

$$\lambda_m = 0.653 \times 10^{-5} \times 760/P \qquad \text{[cm] for air} \qquad (7)$$

These equations contain the slip factor 'Cunningham correction' for

the increase in mean free path of gas molecule and the approximate equation for the drag coefficient of spherical particles.

The simultaneous integro-differential equations (1) and (2) are non-linear, so the analytical solution cannot be obtained. Thus, numerical techniques using a digital computer were employed to obtain the solutions of Eqs. (1) and (2).

Let us now compare two alternative solutions. One is a numerical solution of the simultaneous second-order ordinary differential equations without the last integral terms of Eqs. (1) and (2) by the Runge-Kutta-Merson method. The other is a numerical solution of the integro-differential equations by the methods given in Appendix B.

Strictly speaking, the pressure distribution in the rotor should be considered, but this effect appears to be negligible. The pressure distribution of gas at a constant speed of rotation may be expressed by

$$\frac{dp}{dr} = \frac{\rho_g \, r \, \omega^2}{g_c} \tag{8}$$

For an ideal gas, the general relation between the density and the pressure is

$$\rho_g = p \, \rho_{go} / p_o \tag{9}$$

Substitution of Eq. (9) into Eq. (8) and integration of Eq. (8) with respect to r gives

$$\frac{p}{p_o} = \exp \left(\frac{1}{2} \frac{\rho_{go} \cdot r^2 \omega^2}{p_o \, g_c} \right) \tag{10}$$

using the boundary condition

$$\text{B.C.} \quad \text{at } r = 0,\ p = p_o \tag{11}$$

The calculated pressure distributions are shown in Fig. 4. The deviations of relative pressure p/p_o between outer and inner parts of the rotor are only a few percent.

IV. Experimental Results and Discussion

Figs. 5, 6, and 7 show the comparison of the experimental results and theoretical solutions for glass beads at various pressures and rotor speeds of 3000, 6000, 9000 rpm. Figs. 8 and 9 present the results for zinc powder and glass spheres, respectively.

The solid line represents the numerical solutions computed without the integral term in Eqs. (1) and (2), and the broken line represents the computed values of Eqs. (1) and (2). The solid and broken lines are computed at the following boundary conditions B.C. and initial conditions I.C., respectively.

B.C. $\frac{d\phi}{dt} = \omega$ (const.), that is, the gas rotates at the same angular velocity as the rotor. (12)

I.C. at $t = 0$, $r = r_o$ (13)

$\theta = 0$ (14)

$\frac{dr}{dt} = 0$ (15)

$\frac{d\theta}{dt} = \omega$ (16)

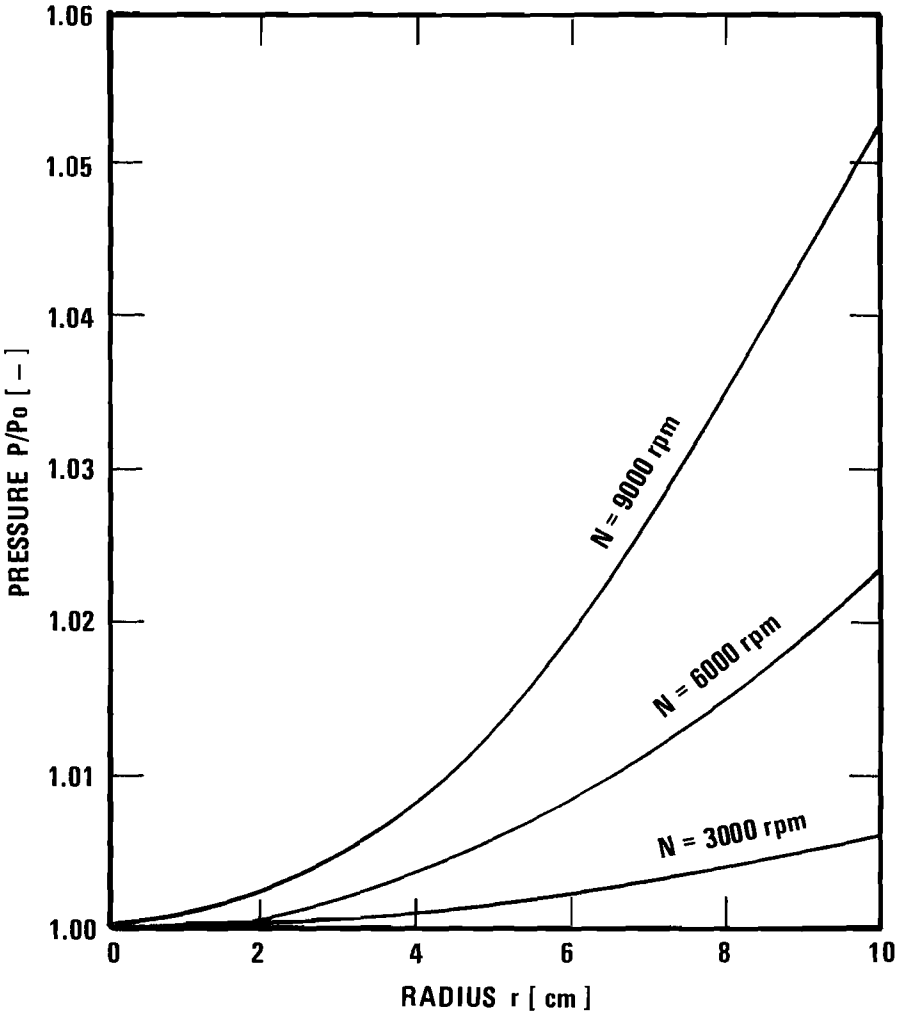

Figure 4. Pressure Distribution in a Gas Centrifuge.

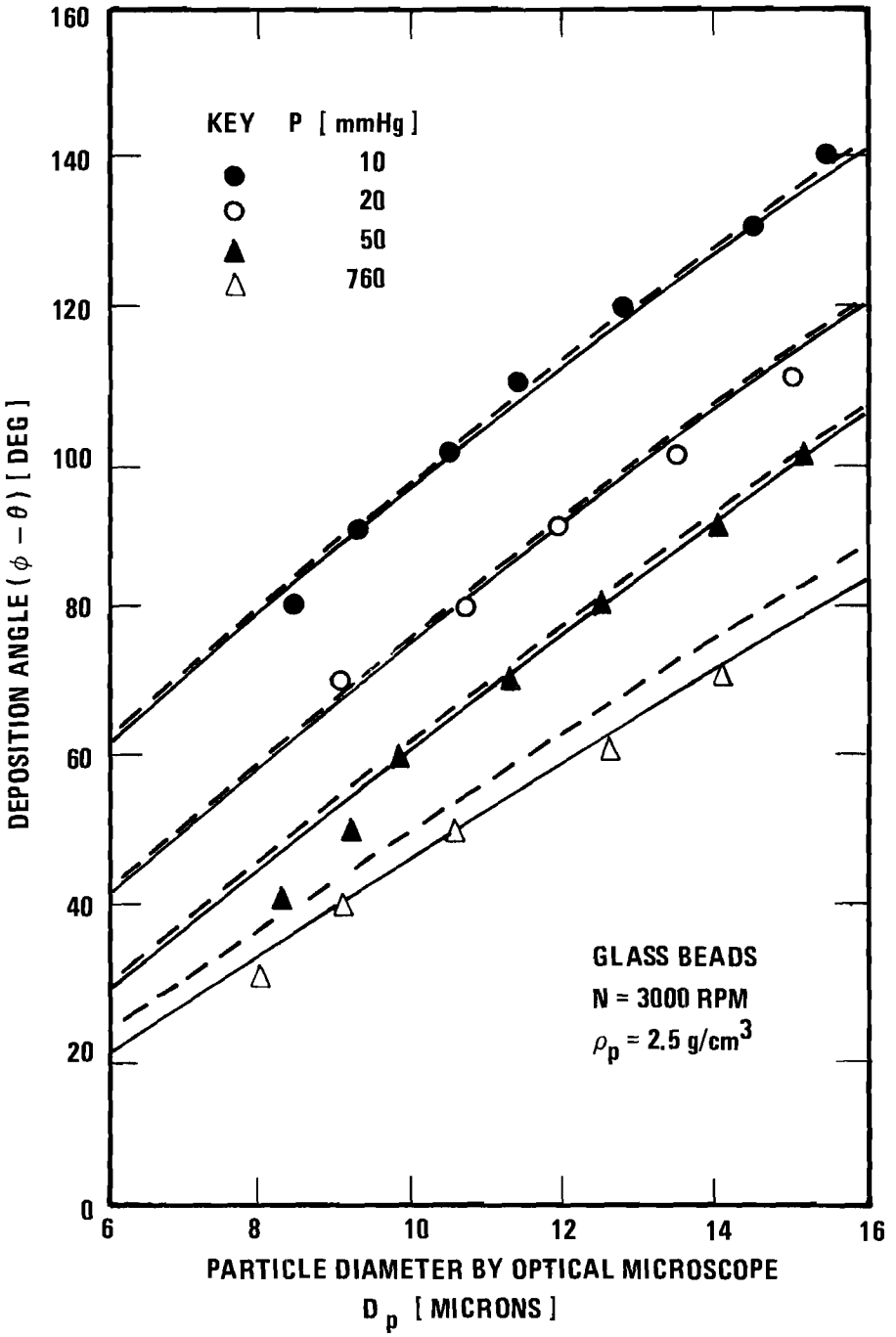

Figure 5. Variation of Deposition Angle with Pressure for Glass Beads (experimental and computed results).

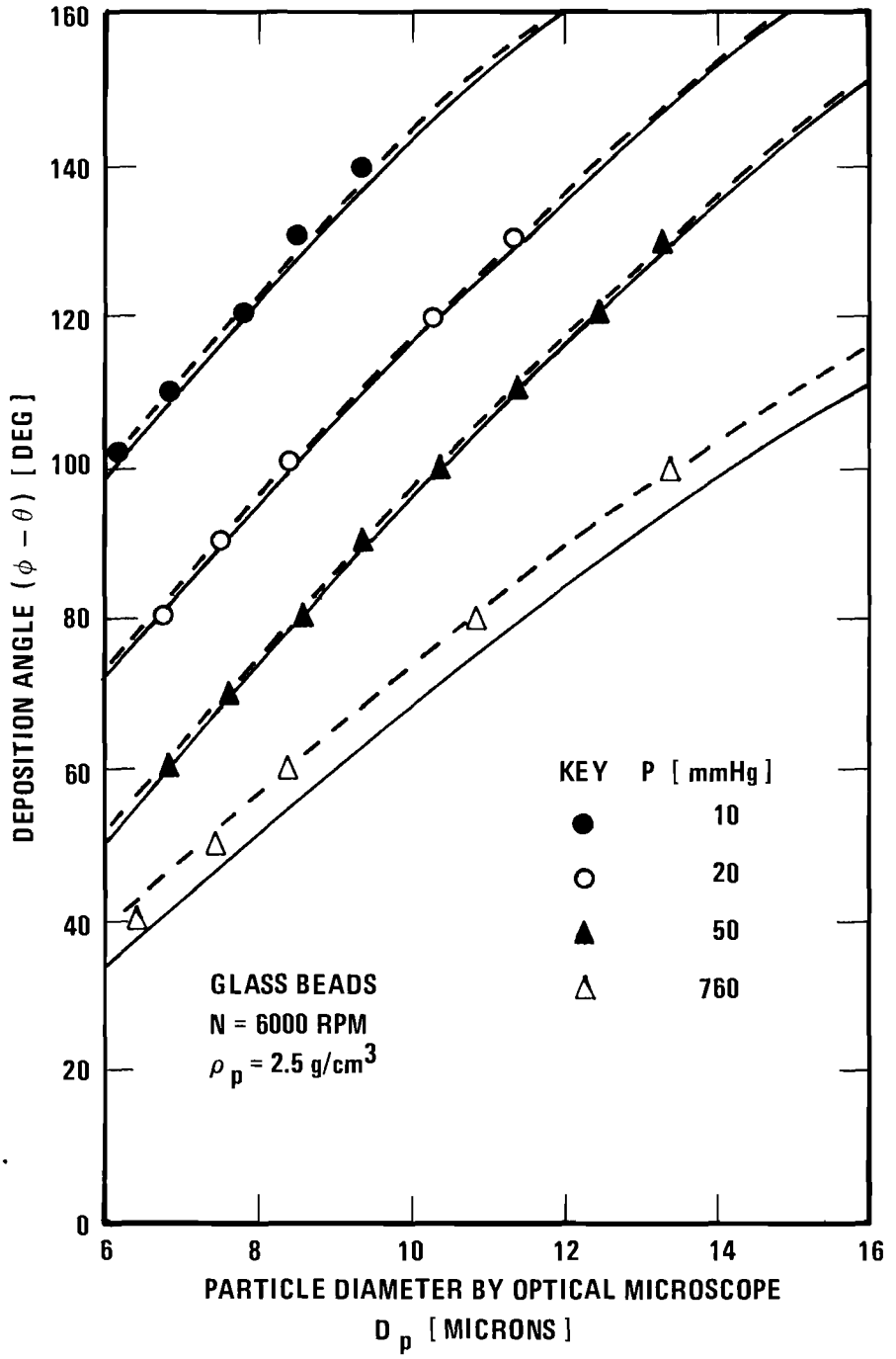

Figure 6. Variation of Deposition Angle with Pressure for Glass Beads (experimental and computed results).

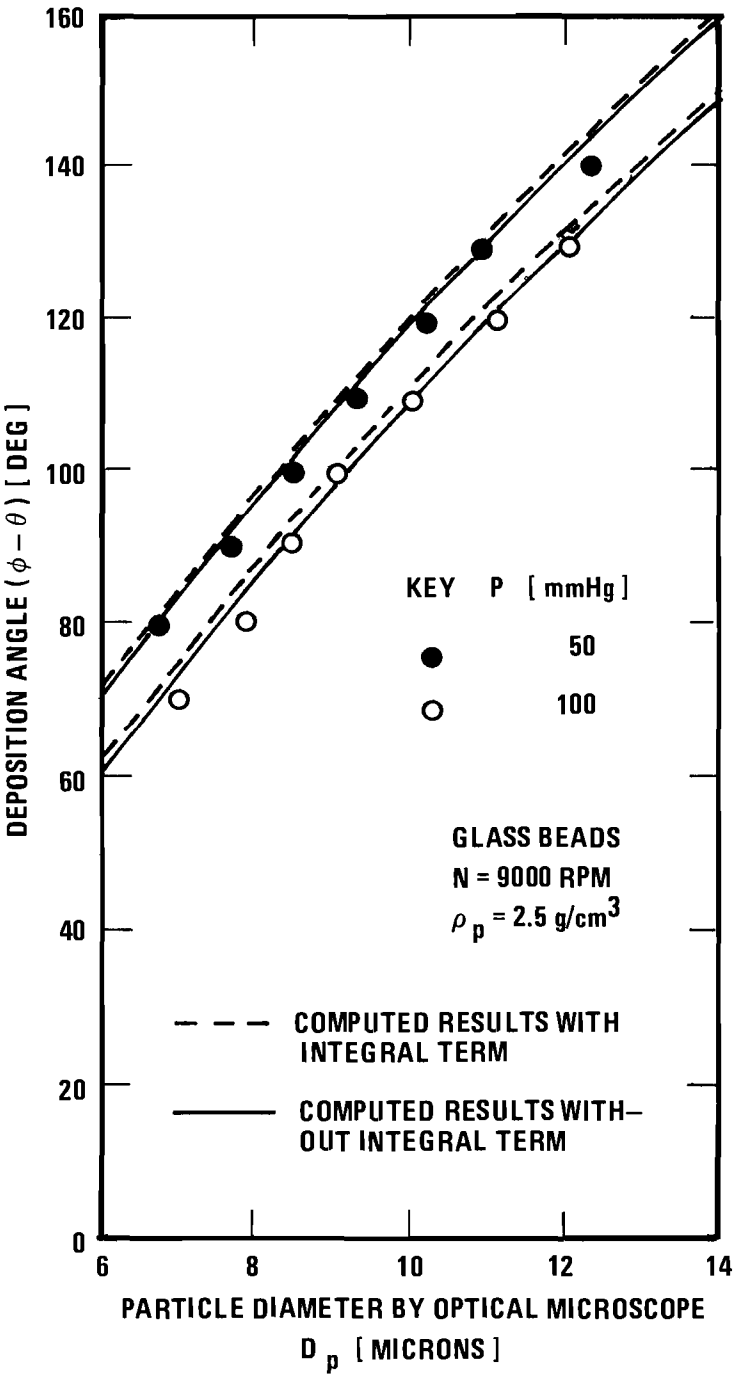

Figure 7. Variation of Deposition Angle with Pressure for Glass Beads (experimental and computed results).

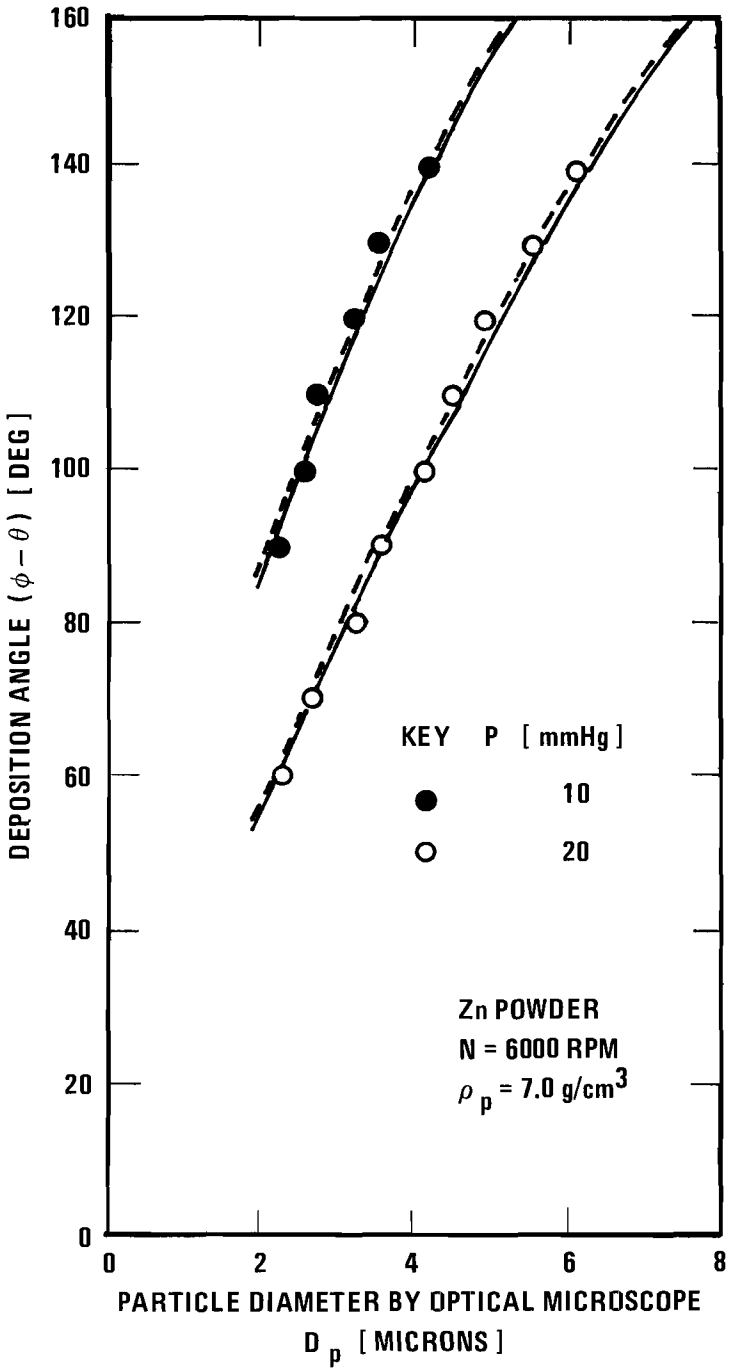

Figure 8. Comparison of Experimental and Computed Results for Zn Powder.

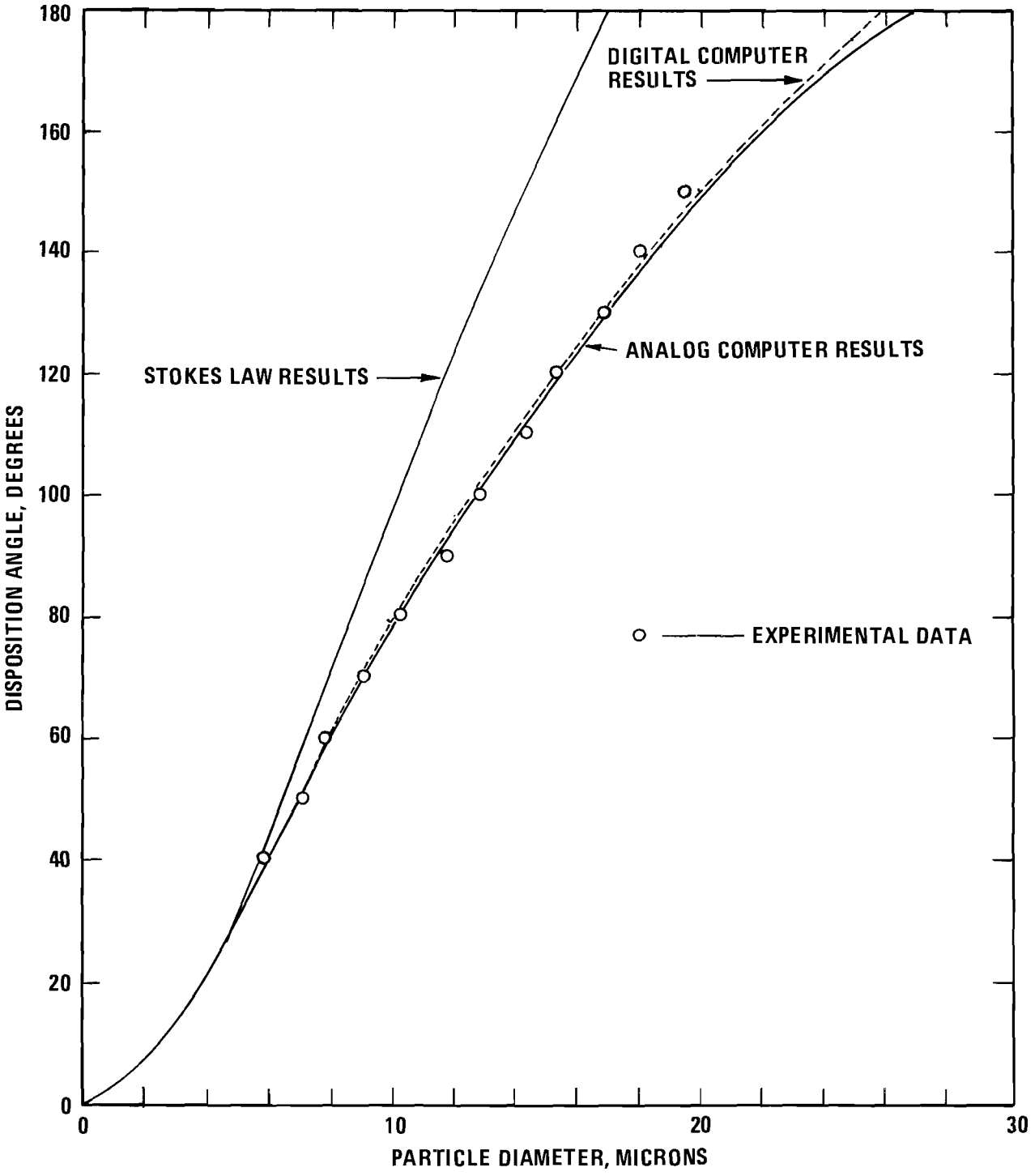

Figure 9. Comparison of Theoretical Solutions with Experimental Data for Glass Spheres (Rotor Speed: 7200 rpm).

The experimental results agree well with the computed values. Figures 10 and 11 show photomicrographs for several experimental runs.

From the numerical calculation, the deposition angle calculated with the integral term included is slightly greater than the value obtained without the integral term and the effect of this term on the calculated value of the deposition angle is less than 10%. Furthermore, the effect decreases with decreasing pressure. Below 20 mmHg the deviation is less than 1%, so the effect of integral term may be considered to be negligible.

If possible, the powder should be fed to the classifier in a well-dispersed aerosol, but the initial radial velocity of the aerosol at the inlet ports reduces the deposition angle. This has been confirmed by both the experimental and theoretical results. Also, it is difficult to insure that the initial radial velocity of each particle is the same. Consequently, this non-uniform velocity may result in decreased classification efficiency. This problem should be given further attention in later studies.

V. Conclusions

Particle size classification in a gas centrifuge at reduced pressure has been investigated theoretically and experimentally, resulting in the following conclusions.

1. Particles down to the submicron size range can be classified with good resolution, a gradation of particle size occurring on the rotor wall.
2. The agreement between the experimental results and the numerical solutions is shown to be excellent.
3. The slip factor 'Cunningham correction' obtained by using Millikan's

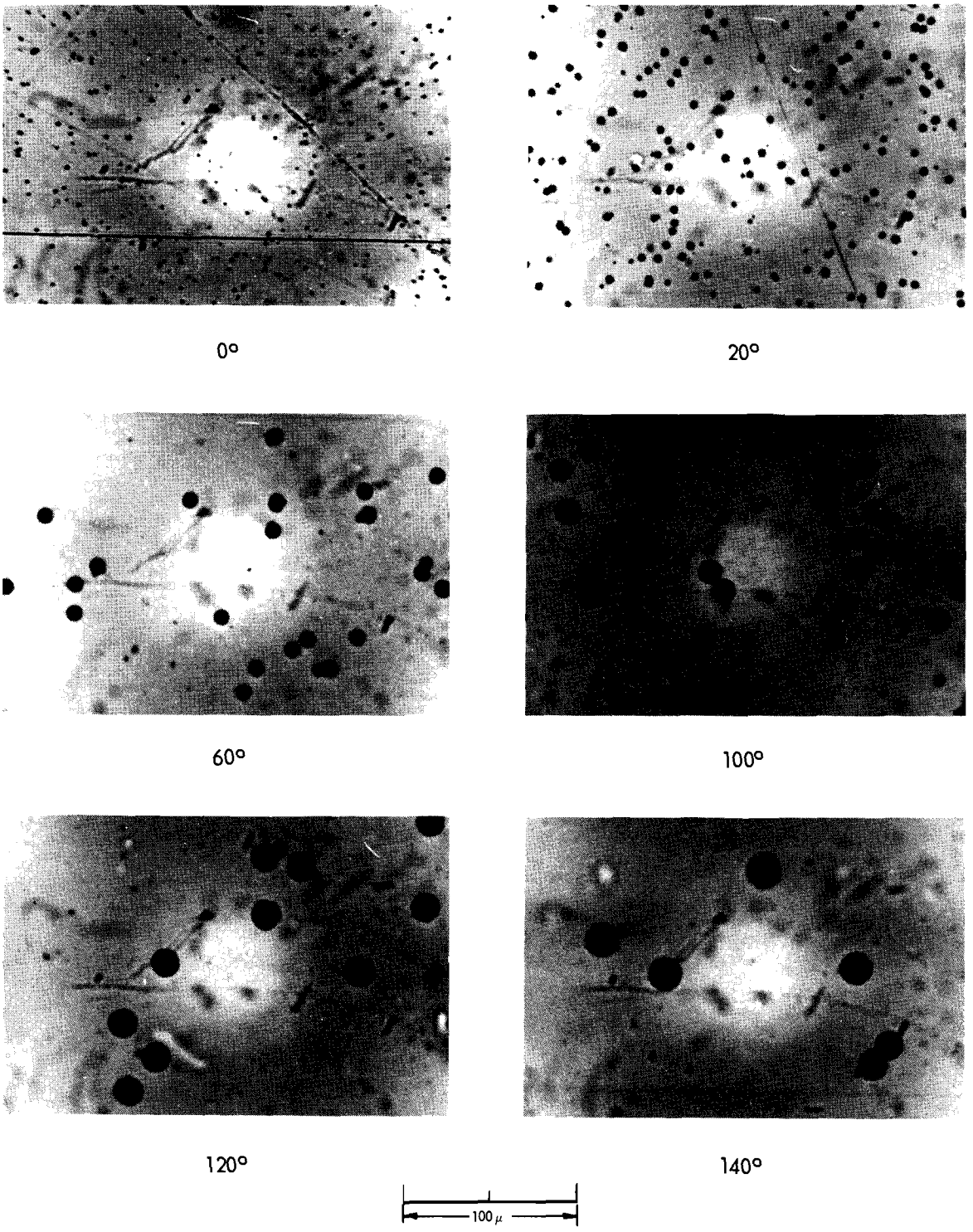

Figure 10. Photomicrographs of Aluminum Particles Collected at Specified Locations in the Centrifugal Classifier Rotor. (Rotor Speed: 7200 rpm).

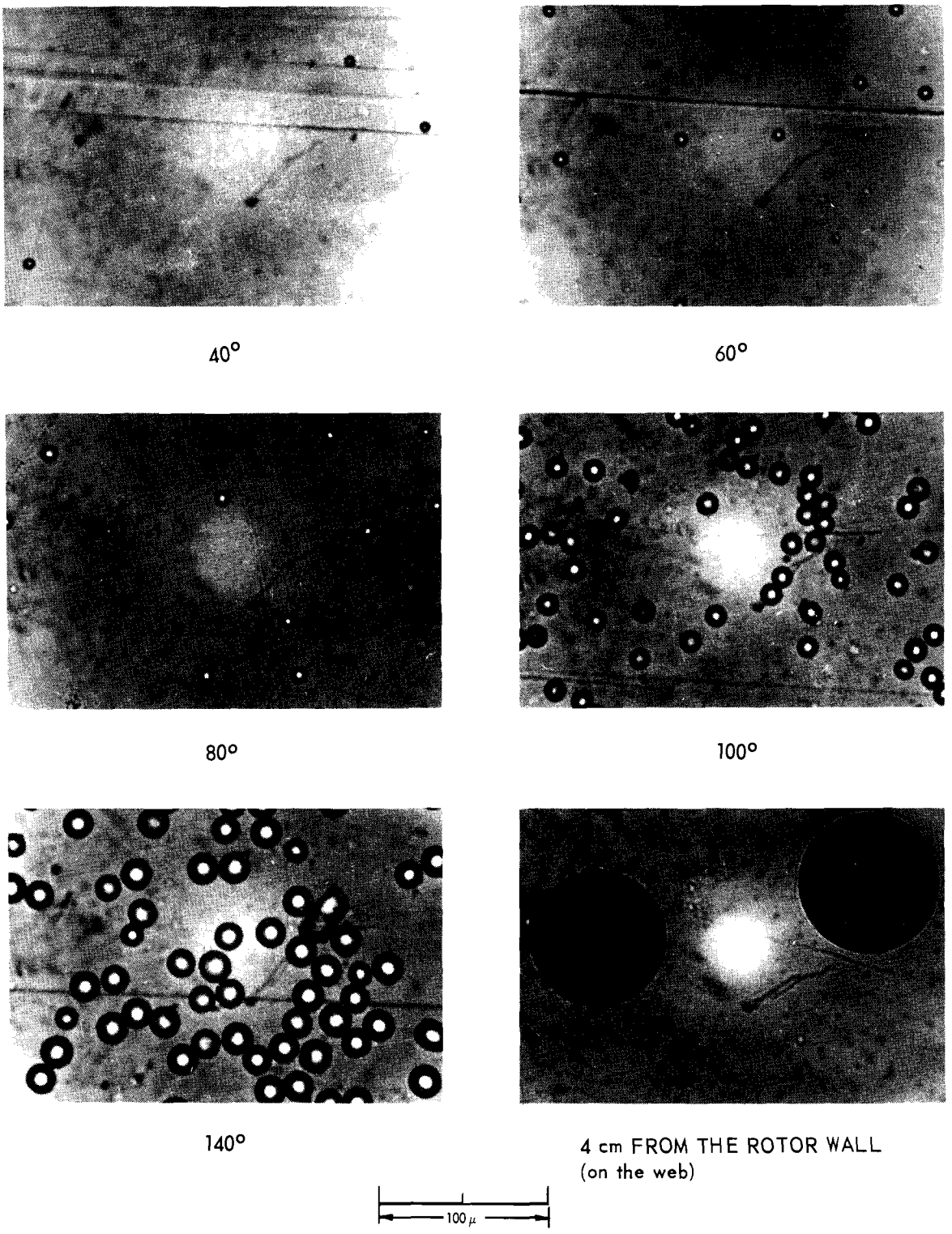

Figure 11. Photomicrographs of Glass Particles Collected at Specified Locations in the Centrifugal Classifier Rotor. (Rotor Speed: 7200 rpm).

data for oil drops in air may be applied to various materials suspended in air and at various pressures.

4. The numerical solutions of the simultaneous integro-differential equations of a non-uniform curvilinear motion have been obtained.
5. The effect of the integral term for fine particles suspended in air is not large.

As a consequence of these results, the development of a new particle size analyser has resulted with many possible applications, particularly in the area of respiratory physiology.

Respectfully submitted,

[redacted]

John H. Burson, III

NOMENCLATURE

C_c	=	Cunningham correction factor	[-]
C_D	=	drag coefficient	[-]
D_p	=	particle diameter	[cm]
g_c	=	gravitational conversion factor	[(g/G)(cm/sec^2)]
N	=	revolution per minute	[rpm]
P	=	pressure	[mmHg]
p	=	pressure	[G/cm^2]
r	=	radius of gyration	[cm]
Re	=	Reynolds number = $(D_p u \rho_g / \mu)$	[-]
t	=	time	[sec]
u	=	relative velocity between particle and fluid in general	[cm/sec]
v	=	relative velocity between particle and fluid defined by Eq. (3)	[cm/sec]
x	=	integral variable	[sec]
θ	=	angular displacement of particle	[rad]
λ_m	=	mean free path of gas molecule	[cm]
ρ_g	=	density of gas	[g/cm^3]
ρ_p	=	density of particle	[g/cm^3]
ϕ	=	angular displacement of gas	[rad]
ω	=	angular velocity of rotor	[rad/sec]

APPENDIX A

T. Yamaoki, "Fractionation by a Modified Elutriation Technique," Masters thesis in Chemical Engineering, Georgia Institute of Technology, 1969.

Z. Tanaka, H. Takai, N. Okada, K. Iinoya and J. Burson, "Particle Size Classification by Deposition Angle in a Gas Centrifuge at Reduced Pressure," Jour. of Chem. Engr. of Japan, 4, 167-171, 1971.

J. Burson, E. Keng, and C. Orr, "Particle Dynamics in Centrifugal Fields," Powder Technology, 1, 305-315, 1968.

J. Burson and K. Iinoya, "Particle Motion in Centrifugal Fields," Japan Jour. Phys. Chem., 6, 137-142, 1971.

J. Burson, "A Centrifugal Particle Analyzer," 19th Southeastern Meeting of American Chemical Society, 137, 1967.

J. Burson, "Centrifugal Particle Classifier for the Sub-Micron Range," 45th National Colloid Symposium, Atlanta, Georgia, June 1971.

K. Iinoya and J. Burson, "Particle Size Analysis with a Gas Centrifuge at Reduced Pressures," Chemical Engineering (Japan), 35, 1041-1046, 1971

Z. Tanaka, K. Iinoya and J. Burson, "New Approximate Equation of Drag Coefficient for Spherical Particles," Jour. of Chem. Engr. of Japan, 3, 261-262, 1971.

Z. Tanaka, K. Iinoya and J. Burson, "A Method to Assess Particle Size Classification Efficiency," Jour. of Chem. Engr. of Japan, 2, 259-261, 1971.

J. Burson, "Particle Dynamics in Centrifugal Force Fields," Georgia Institute of Technology, Ph.D. Thesis, 1964.

APPENDIX B

The calculation of the integral term is carried out using the relative velocity between the particle and the fluid, u, to simplify the notation.

The first stage of average acceleration is defined by

$$\left(\frac{du}{dt}\right)_{lm,1} = \tfrac{1}{2}\left\{\left(\frac{du}{dt}\right)_0 + \left(\frac{du}{dt}\right)_{1,1}\right\} \tag{1a}$$

in which $(du/dt)_{i,j}$ denotes j-th approximation of i-th step and the subscript m denotes the mean value. The first approximation of the integral term after a small increment of time Δt is

$$\int_0^{\Delta t} \frac{\frac{du}{dx}}{\sqrt{\Delta t - x}}\, dx = 2\left(\frac{du}{dt}\right)_{lm,1} \sqrt{\Delta t} \tag{2a}$$

Substituting Eq. (2a) in Eqs. (1) and (2), the second approximation $(du/dt)_{1,2}$ can be calculated. Then from Eq. (1a), $(du/dt)_{lm,2}$ may be evaluated. If the n-th approximation is nearly equal to the (n-1)-th approximation

$$(du/dt)_{1,n} - (du/dt)_{1,n-1} = \text{tolerance limit} \tag{3a}$$

Then defining the final approximation of the first step

$$(du/dt)_1 = (du/dt)_{1,n} \tag{4a}$$

and the mean acceleration $(du/dt)_{lm}$ is calculated.

Thus from Eq. (2a), the value of the integral term at the end of the first increment of time can be evaluated. Similarly, $(du/dt)_{im}$ and the integral term can be calculated. For the purpose of calculation, the time is divided into k steps (it is not necessary that each step is an equal interval) and the integral term is computed as follows:

$$\int_0^t \frac{\frac{du}{dx}}{\sqrt{t-x}}\,dx = 2\sum_{i=1}^{k} (du/dt)_{im}\,\{\sqrt{t-x_{i-1}} - \sqrt{t-x_i}\} \qquad (5a)$$

Applying this method to the radial and angular directions, the numerical integration of Eqs. (1) and (2) by the RKM method gives the required results.